

Research Article

Influence of Hydrogen Content on the Microstructure and Mechanical Properties of ER5183 Wires

Yilong Han,¹ Songbai Xue ,¹ Renli Fu,¹ Lihao Lin,² Zhongqiang Lin,² Yinyin Pei,³ and Huawei Sun³

¹College of Materials Science and Technology, Nanjing University of Aeronautics and Astronautics, Nanjing 210016, China

²Zhejiang Yuguang Aluminum Material Co. Ltd., Jinhua 321200, China

³State Key Laboratory of Advanced Brazing Filler Metals & Technology, Zhengzhou Research Institute of Mechanical Engineering, Zhengzhou, China

Correspondence should be addressed to Songbai Xue; xuesb@nuaa.edu.cn

Received 13 December 2018; Accepted 21 March 2019; Published 3 April 2019

Academic Editor: Stanislaw Dymek

Copyright © 2019 Yilong Han et al. This is an open access article distributed under the Creative Commons Attribution License, which permits unrestricted use, distribution, and reproduction in any medium, provided the original work is properly cited.

This work focused on the influence of hydrogen content on the microstructure and mechanical properties of ER5183 Al-Mg-Mn alloy wires for aluminum alloy welding. The hydrogen content of the ER5183 wires was measured, the macroscopic and microscopic morphologies of fractures were observed as well as the microstructure of the wires, and the tensile strength of the wires was also tested and investigated. The experimental results demonstrated three typical irregular macroscopic fractures of the wires appeared during the drawing process when the hydrogen content exceeded $0.23 \mu\text{g/g}$. In the meantime, the aggregated pores were observed in the microstructure of the $\phi 5.2$ mm wire with the hydrogen content of $0.38 \mu\text{g/g}$. Such defects may become the origin of cracks in subsequent processing and tensile tests. Moreover, higher hydrogen content in the $\phi 5.2$ mm welding wire will bring obvious changes in the fracture surface, which are internal cracks and micropores replacing the original uniform and compact dimples. With the higher hydrogen content, the tensile strength and plastic strain rate of $\phi 1.2$ mm wires would decrease. At the same time, unstable crack propagation would occur during the process of plastic deformation, leading to fracture. Considering the mechanical properties and microstructure, the hydrogen content of the ER5183 wires should be controlled below $0.23 \mu\text{g/g}$.

1. Introduction

Aluminum alloys have a wide application prospect in the field of automobile manufacturing and high-speed railway due to the advantages of light density, excellent corrosion resistance, easy processing, etc. [1–3]. Aluminum alloys have attracted widespread attention and became a new generation of structural materials in place of ferrous metal [4]. In recent years, as a widely used high-strength welding material as well as the better performance in mechanical properties than ER5356, ER5183 wires play a crucial part in the reliability of aluminum alloys structural materials and are frequently used in automatic and semiautomatic GMAW (gas metal arc welding) which requires good property of wire-feeding and appearance of welding [5]. Compared with other gas elements like O, N exists in the welding atmosphere and H has the highest dissolvability in aluminum alloys, which makes it

the major gas element that dissolves in ER5183 wires during the solidification process [6]. As a result, the microporosities and cracks are detected in the matrix of aluminum alloys semimanufactured rods [7]. Therefore, the investigation on the formation mechanism of hydrogen-induced porosities and cracks in the microstructure is important to the production of qualified ER5183 wires. It is well known that a stable process is the key factor of homogeneous microstructure which is the quality guarantee of the wire-feeding property. But the porosities and cracks may cause the stress concentration under the external load and affect the homogeneity of the wires. Finally, in the situation of finished products, the combined effect of stress concentration, microcracks, and porosities worsen the mechanical properties of finished products [8]. Therefore, research on the influence of the hydrogen content of ER5183 wires is urgent and necessary.

Hydrogen is a common impurity that affects the microstructure as well as mechanical properties of aluminum alloys and other metals, and there were some issues about the influence of hydrogen. Lu et al. studied the properties of dislocation core with and without H impurity using the Peierls–Nabarro model. The results showed that H has the ability of facilitating the emission of dislocation from the tip of cracks; in the meantime, they enhance the mobility of the dislocation dramatically. As a result, the macroscopically softening as well as the thinning ahead of the crack tip appeared. Besides, strong binding was observed between dislocation cores and H which inhibits dislocation cross-slip and develops slip planarity to affect the mechanical property of aluminum [9]. The hydrogen content of aluminum alloys can be largely affected by the environmental humidity. Gou et al. analyzed the welded joints obtained under various humidity conditions using A7N01S-T5 aluminum alloy and found the similarity of the microstructures in both the HAZ (heat-affected zone) and the weld zone. Furthermore, the distribution of porosity was significantly affected, and the quantity of porosity increased cooperating with the humidity. Besides, the joint showed brittle fracture made under the 70% humidity while others showed ductile fracture. The result demonstrated that 70% humidity has a great possibility to be the limit humidity level for welding [10]. Lu et al. found that hydrogen could cause the embrittlement in bulk aluminum under the specified condition. Vacancies could compensate the energy cost by combining with hydrogen impurities to form the defect. Three nearest single vacancies would aggregate and repel to form a trivacancy on the slip plane of aluminum with the presence of trapped H atoms. These vacancies could act as a birthplace for cracks and microvoids which result in the ductile fracture along the planes [11]. The porosity of narrow-gap GMAW was analyzed by Zhu et al. using the 5083 aluminum alloy thick plate. The hydrogen was found to be the major cause of the porosity. They adjusted heat input using the optimized parameters to avoid pores and reduce the influence of hydrogen [12]. In consideration of hydrogen is the major active gas element leading to porosity in aluminum alloys, Obaldia et al. calculated the volume fraction of hydrogen-induced microporosity in castings of A356 aluminum alloy by extending a model of dendritic solidification. The simulation results are consistent with the experimental data. An online approach was also used by Yu et al. to analyze the hydrogen porosity in pulsed gas tungsten arc welding of the Al-Mg alloy. Spectral lines of H and Ar components among the arc atmosphere were analyzed, and they successfully identified the position with most probable of the native porosity and the exact position of the artificial porosity [13]. The grain size was chosen as a factor by Chou et al. to study the resistance of duplex stainless steel to hydrogen-assisted crack. The results indicated that finer grain size can decrease the susceptibility to hydrogen embrittlement and increase the tensile strength and uniform elongation of duplex stainless steels [14].

A lot of work researched the influence of hydrogen on aluminum alloys. However, very few studies focused on the microstructure and mechanical properties of aluminum

alloys welding wires which are the crucial factors for the performance of aluminum welding consumable and reliability of aluminum alloy structure. Therefore, the ER5183 aluminum alloy wires were chosen in this work, and the influence of the hydrogen content was discussed. The hydrogen content was measured for quantitative analysis. The macroscopic morphologies of the drawing fracture were observed to identify the mode of fracture and analyze the influence of the hydrogen content on mechanical properties. The microscopic morphologies of the fracture and wire matrix were chosen to further research on the fracture mechanism and the role that hydrogen played. The tensile strength of both the semifinished products and the finished products was measured to study the influence of the hydrogen content on mechanical performance. The results demonstrated the influence of hydrogen on the microstructure and mechanical properties of ER5183 wires, and the recommended content was proposed.

2. Experimental Procedure

2.1. Production and Hydrogen Test of ER5183 Wires. Firstly, metal ingots and additives were used for the smelting of ER5183 wires. Subsequently, in order to remove hydrogen which is abundant in raw materials, the melt was refined with hexachloroethane (C_2Cl_6) and pure argon (99.99%). To determine the residual hydrogen content, the hydrogen test specimens were obtained from $\phi 5.2$ mm semifinished wires and measured by the hydrogen analyzer LECO RHEN602. The schematic diagram of the hydrogen testing sample is shown in Figure 1. The finishing machining was drawing-shaving to prepare the $\phi 1.2$ mm wires. The chemical compositions of wires which measured by the SPECTRO MAXx04D spectrometer are listed in Table 1. The wires accord with the European standard EN 14532-3: 2004.

2.2. Tensile Test of ER5183 Wires. After the hydrogen test, the tensile test of ER5183 $\phi 5.2$ mm semifinished wires was performed on a WDW-20E electronic universal testing machine (Zhejiang Jingyuan Mechanical Equipment Co., Ltd.) which operated at room temperature. After that, the samples were made into $\phi 1.2$ mm products, and the tensile strength was tested again. The test data were obtained from three specimens and averaged.

2.3. Observation of Fracture Morphologies and Microstructure. The stereoscopic microscope was used to observe the macromorphologies of the $\phi 5.2$ mm semifinished product samples after tensile tests. The fracture morphologies and the microstructure were observed and analyzed by OM (Zeiss Axio Vert A1) and SEM (ZEISS SIGMA field-emission scanning electron microscope).

3. Results

3.1. Hydrogen Content of $\phi 5.2$ mm Wires and the Fracture during Processing. The hydrogen content of $\phi 5.2$ mm wires is shown in Table 1. The hydrogen content ranges from

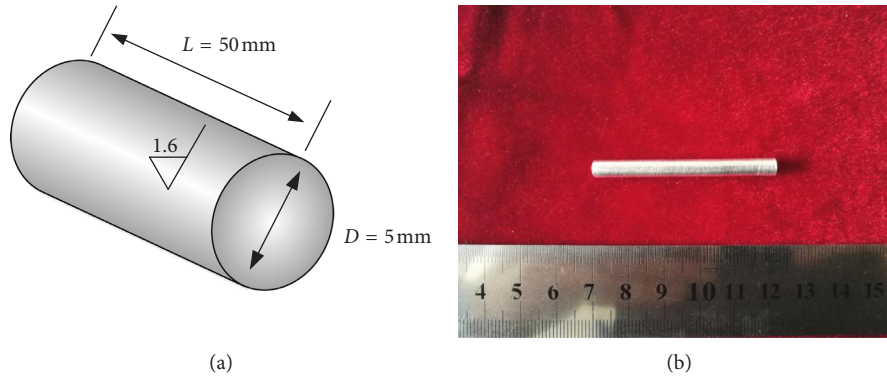


FIGURE 1: Schematic diagram and macroscopic view of the hydrogen testing sample.

TABLE 1: Chemical compositions of wires (wt.%).

No.	H ($\mu\text{g/g}$)	Si	Fe	Mg	Mn	Cr	Ti	Al
1	0.18	0.062	0.138	4.73	0.78	0.104	0.125	Bal.
2	0.23	0.061	0.136	4.73	0.78	0.110	0.132	Bal.
3	0.26	0.064	0.136	4.72	0.75	0.106	0.131	Bal.
4	0.32	0.063	0.140	4.74	0.75	0.108	0.132	Bal.
5	0.38	0.062	0.138	4.72	0.78	0.109	0.128	Bal.

0.18 to 0.38 $\mu\text{g/g}$ which were obtained from 5 samples correspondingly. Figure 2(a) shows the process that the wire passes through the drawing die. When the wire reaches the contact position with the drawing die, the influence of the triaxial stress brings a great test of the mechanical property of the wires. The wire with the low hydrogen content (lower than 0.23 $\mu\text{g/g}$) occasionally breaks due to the issue of the production equipment and shows a ductile fracture surface in Figure 2(b) with a neck. Besides, the microstructure of the wire is homogeneous which maintains the stability during the drawing process. In the meantime, the homogeneous structure of the wires can effectively reduce the resistance of the drawing die to the wires and improve the quality of the wire surface.

In contrast, three typical modes are observed in the irregular fracture surface of the wires with the high hydrogen content (higher than 0.23 $\mu\text{g/g}$):

Mode I (Figure 3(a)): due to the continuous applied load during drawing processing, a stripped layer forms outside the core of the wire. As a consequence, this kind of weak structure results in the stripped skin (Figure 3(b)) under the extrusion and drawing force of the die at the contact position. Mode II (Figure 3(c)): some internal cracks (Figure 3(d)) were formed inside the wire under the applied load. Moreover, with the further deformation, those cracks decrease the continuity of the wire which reduces the effective loading area and finally cause the fracture. Mode III (Figure 3(e)): hydrogen concentrates in a certain part of the wire; as a result, defects were found both on the surface and the internal structure. Subsequently, cracks are formed at the defect, and the cracks propagate along the damaged structure, penetrating both the surface and the interior (Figure 3(f)). The fracture is dim and irregular. In addition, scratches were observed on the surface, which were caused

by the resistance between the damaged tissue and the drawing die.

The molten aluminum alloy is easy to absorb gas especially vapor which contains plenty of hydrogen during the smelting process. Some H atoms are dissolved into interstitial positions in the Al matrix and trapped at vacancies. As a consequence of H trapping, the formation energy of the vacancy defect is lowered significantly, which can result in increasing in vacancy concentrations. In turn, the superabundant vacancy formation provides more trapping sites for H impurities, which effectively increases the tendency of H aggregating in bulk Al [11].

3.2. Aggregated Pores on the Microstructure of $\phi 5.2$ mm Wire. EDX element mappings of the microstructure of the $\phi 5.2$ mm wire with the hydrogen content of 0.38 $\mu\text{g/g}$ are shown in Figure 4. The aggregated pores and the white Al-Mg-Mn-Fe phase were observed. Formation of the pores is caused by the difference of the solubility of hydrogen between the solid and liquid aluminum. During the solidification of the processing, the solubility of atomic H decreases greatly. As a result, the dissolved atomic H aggregates to the H_2 molecule to escape but blocked by a rapid cooling process. The H_2 molecule unable to escape may cause the porosity. Moreover, some pores will aggregate to each other as a consequence of plastic deformation, which is shown in Figure 4(g). In the subsequent process, under the action of axial tension, the radial compression deformation occurs, and the adjacent pore gradually approaches each other, eventually joining each other to form the "aggregated pores" defect. Simultaneously, microcracks are formed around the defects. Such defects may be the origin of cracks in subsequent processing and tensile tests.

3.3. Influence of Hydrogen Content on the Tensile Strength and the Fracture of $\phi 5.2$ mm Wires. Figure 5 reveals that there has been a gradual decline in the tensile strength of the $\phi 5.2$ mm wires with the increase of the hydrogen content. In the samples with 0.18 and 0.23 $\mu\text{g/g}$ hydrogen content, the latter exhibits less than 3 MPa drop in tensile strength, which means the hydrogen has not yet given an obvious impact on the mechanical performance of the wires. However, as the

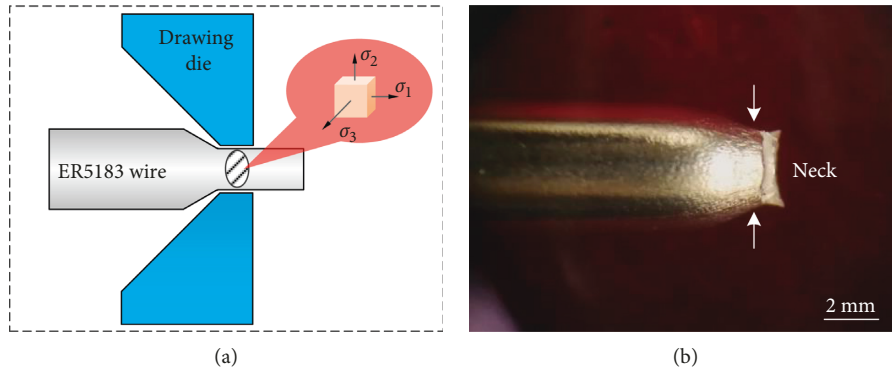


FIGURE 2: The $\phi 5.2$ mm wire in drawing processing and the macroscopic fracture of wires with low hydrogen content: (a) contact between drawing die and $\phi 5.2$ mm wire; (b) necking phenomenon of the $\phi 5.2$ mm with hydrogen content of $0.18 \mu\text{g/g}$.

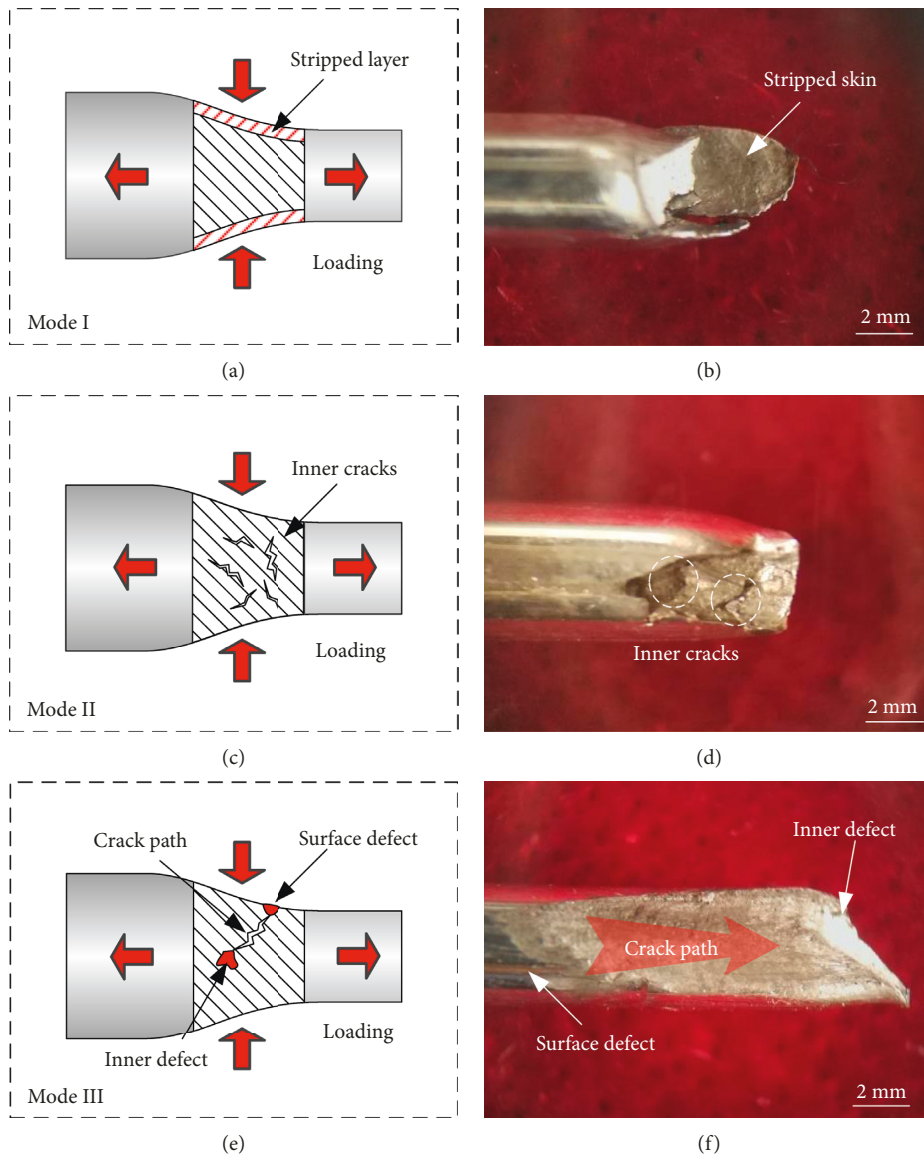


FIGURE 3: Schematic diagram and macroscopic morphology of three fracture modes: (a) Model I: stripped layer; (b) macroscopic fracture corresponding to (a); (c) Model II: internal cracks; (d) macroscopic fracture corresponding to (c); (e) Model III: crack penetrating the surface and the interior; (f) macroscopic fracture corresponding to (e).

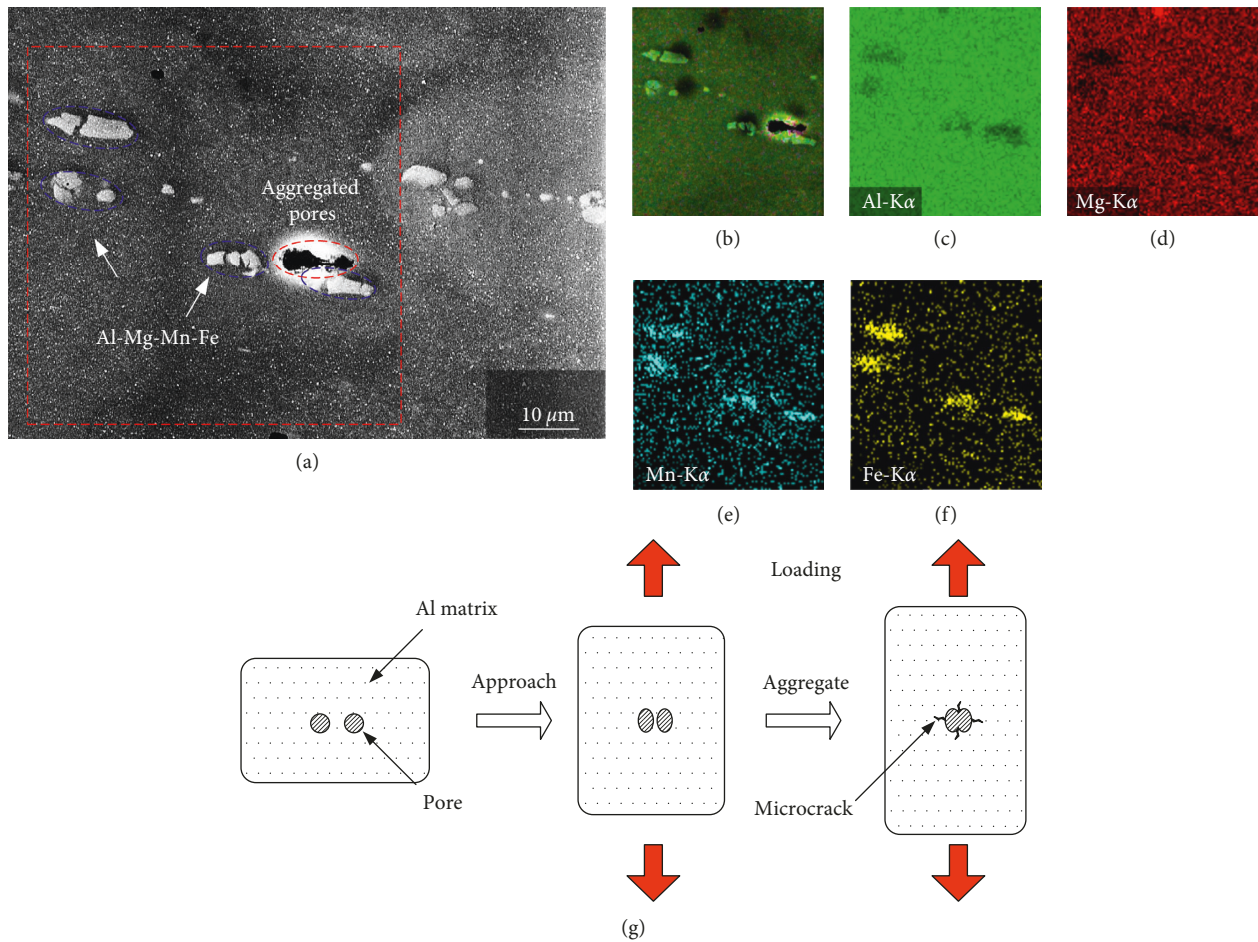


FIGURE 4: The aggregated pores in the matrix of $\phi 5.2$ mm wire: (a) SEM micrograph of the aggregated pores; (b) EDX element mappings; (c)–(f) the distribution of Al, Mg, Mn, and Fe, respectively; (g) schematic diagram of the aggregated pores.

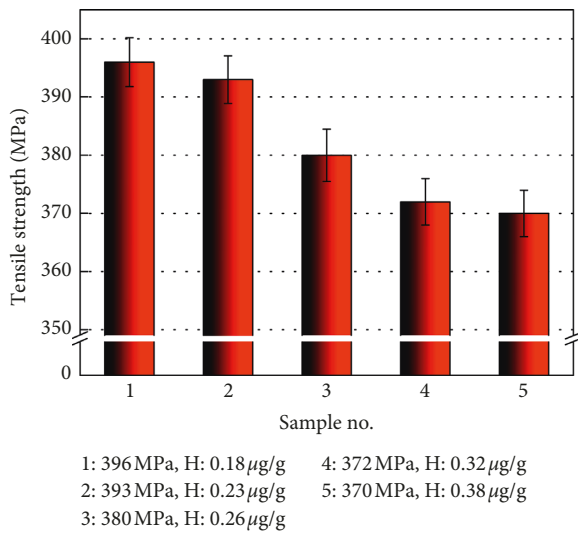


FIGURE 5: Tensile strength of the $\phi 5.2$ mm wires.

hydrogen content increases, a marked drop turns up in the samples with the hydrogen content higher than $0.23 \mu\text{g/g}$. Compared to sample 1, with the hydrogen content of $0.26, 0.32,$ and $0.38 \mu\text{g/g}$, respectively, the tensile strength of

samples 1, 2, and 3 decreases by 16, 24, and 26 MPa. This kind of drop in the tensile strength reflects the change of the microstructure of the wires and may cause potential negative impact on the final performance.

The microscopic fracture surface of the $\phi 5.2$ mm wires after the tensile test was chosen for further observation. In the sample with the low hydrogen content, fractures with necking and less defects are found in Figure 6(a). In the high magnification (Figure 6(b)), the morphology mainly consists of dimples with second-phase particles. Figure 6(c) shows the case of low hydrogen content. Under the action of external loading, the necking phenomenon begins to occur in the tensile specimens, which results in the triaxial stress in the necking region. The crack nucleation and propagation will not be disturbed by hydrogen, but present a smooth process.

With the increase of the hydrogen content, the fracture surface presents an irregular and coarse appearance shown in Figure 7(a). In the high magnification image (Figures 7(b) and 7(c)), cracks with different orientation were observed, respectively. Figure 7(d) reveals the details of the fracture process. Some internal cracks are thought to originate in H-rich zones. These H-rich zones are generated by a critical local concentration of H. Excess hydrogen can promote

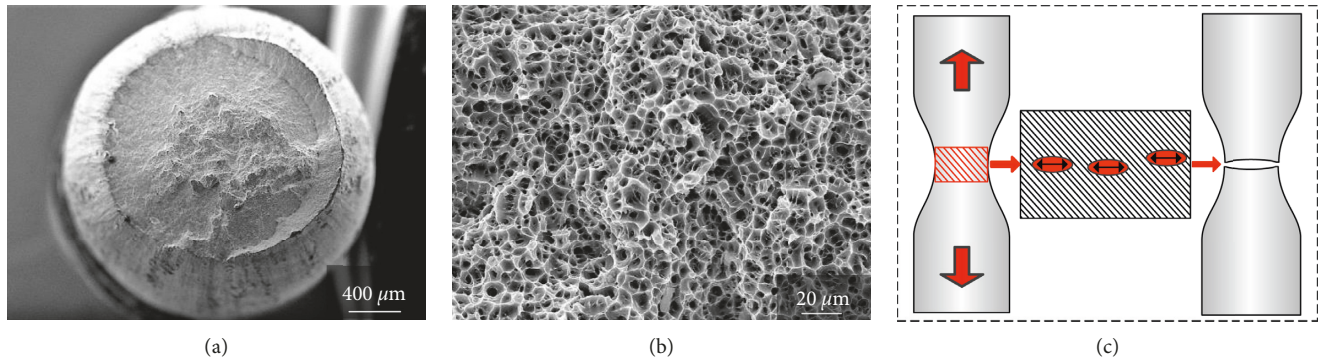


FIGURE 6: The fracture morphology of the $\phi 5.2$ mm wire with hydrogen content of $0.23 \mu\text{g/g}$: (a) macroscopic morphology of the fracture; (b) microscopic view of the dimples; (c) schematic diagram of the regular fracture.

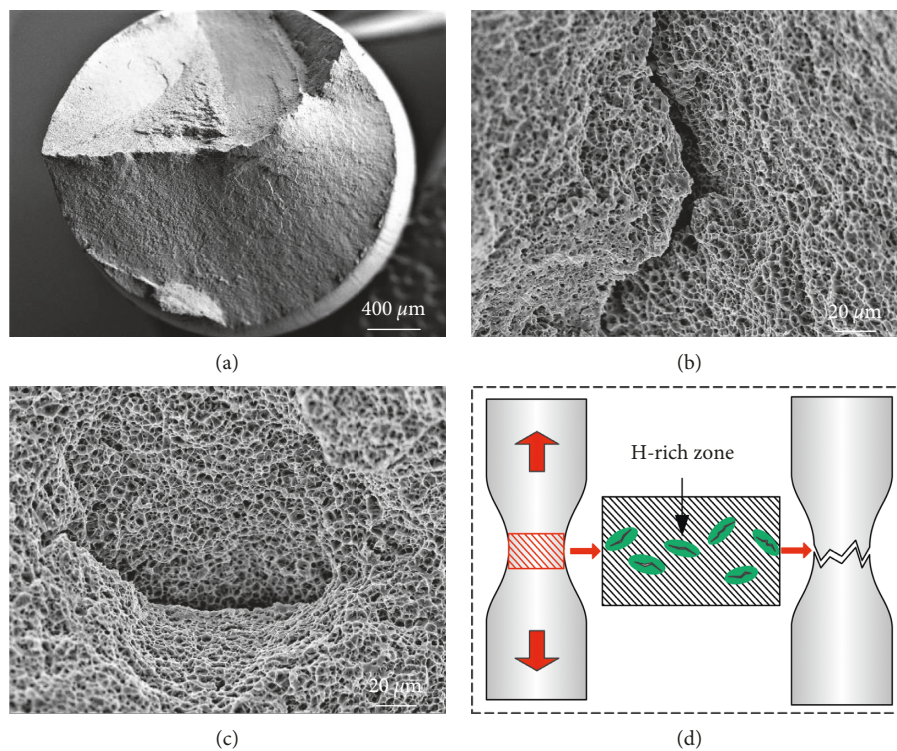


FIGURE 7: The fracture morphology of the $\phi 5.2$ mm wire with hydrogen content of $0.26 \mu\text{g/g}$. (a) Macroscopic morphology of the fracture; (b) and (c) microscopic view of the internal cracks; (d) schematic diagram of the H-rich zone and internal cracks.

dislocation movement in the process of lattice motion. Therefore, under the external load in the processing, the cracks can easily propagate along the newly generated slip plane. Subsequently, some internal defects begin to emerge, forming fragile areas. The fragile areas with more defects will break directly in the processing. At the same time, some defects will be retained, which will affect the mechanical properties of the wire in the tensile test.

Secondary cracks accompanied by some black spots appeared at the fracture and in the sample with hydrogen content of $0.38 \mu\text{g/g}$, is shown in Figure 8(a). In the high magnification image (Figure 8(b)) of section A, the intersection of the crack propagation plane is observed. The appearance of this morphology is mainly due to the

initiation of a new slip system under the influence of hydrogen, which results in a change in the direction of crack propagation. Besides, in the high magnification image (Figure 8(c)), the black spots are identified as some oval-shaped pores on the fracture surface which formed during the solidification and remained in the matrix of the wire. In the process of fracture (Figure 8(d)), the pores lead to the formation of cracks; then, these cracks interconnected to form fracture surfaces.

The wires containing higher hydrogen can generate more initial micropores. With the plastic deformation of the wire during the drawing process, the structure around the pores deteriorates. Besides, hydrogen can weaken the bonding between Al atoms which drove the formation of

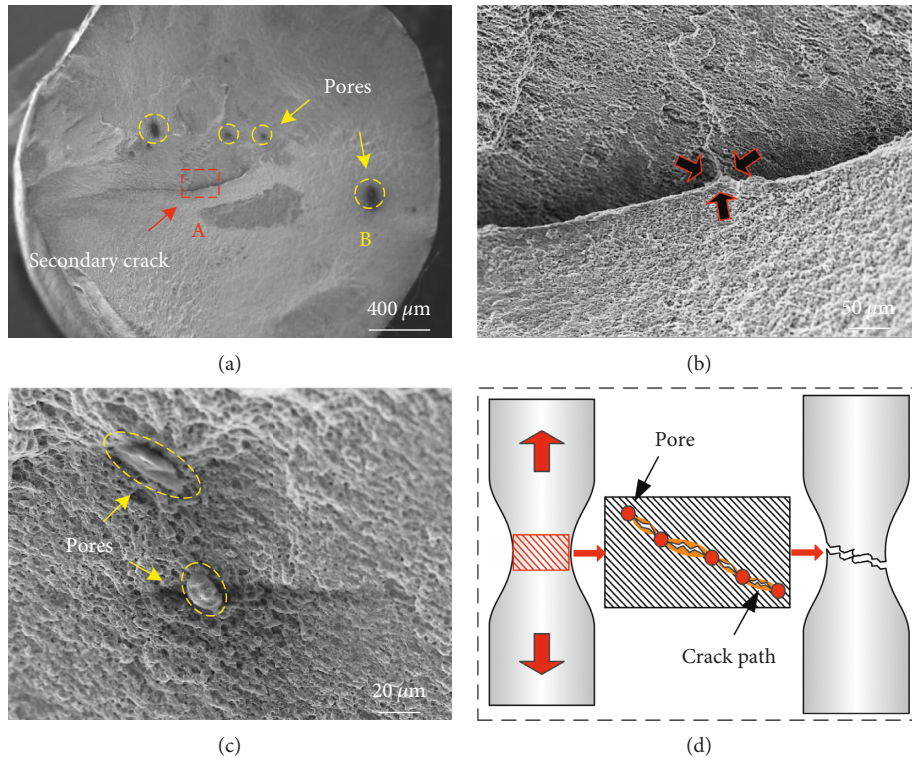


FIGURE 8: The fracture morphology of the $\phi 5.2$ mm wire with hydrogen content of $0.38 \mu\text{g/g}$. (a) Macroscopic morphology of the fracture; (b) and (c) microscopic view of the fracture surface; (d) schematic diagram of pores leading to the formation of cracks.

the multivacancies [11]. During the plastic deformation, vacancies could affect the slip of crystal and dislocation and then generate new glide planes to avoid the obstruction. The more hydrogen the wire had, the more irregular morphology the fracture had.

3.4. Influence of Hydrogen Content on the Tensile Properties of $\phi 1.2$ mm Wires. The stress-strain curves of $\phi 1.2$ mm wires are shown in Figure 9. It is apparent from this figure that, with the increase of the hydrogen content, the tensile strength and plastic strain of the wire decrease. The $\phi 1.2$ mm wires had large deformation through the whole process. The relatively higher hydrogen content (0.26 – $0.38 \mu\text{g/g}$) could generate more microdefects in the wires. When microdefects present in a tensile sample, they will concentrate the stress and become the origin crack source to reduce the load-bearing area. Reflected in macroperformance, the tensile strength decreases. Moreover, the effect of Portevin–Le Chatelier (PLC) which shows as sawtooth stress yielding phenomenon is observed in those tensile specimens. The PLC effect is considered to be caused by the dynamic interaction between the micromovable dislocation and the solute atoms [15]. When the lattice motion cannot continue in the one slip system, another slip system will start, which results in the sawtooth stress yielding. In the samples with low hydrogen content, this kind of yielding phenomenon can proceed smoothly. In contrast, due to the promotion of hydrogen on the dislocation movement, the fracture process will not absorb much energy, thus reducing the ultimate

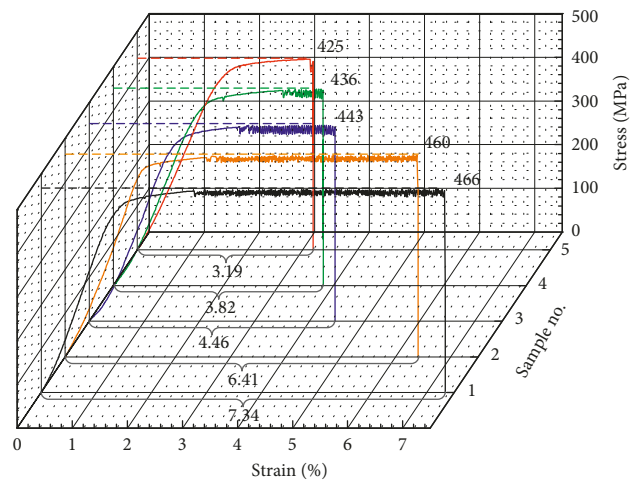


FIGURE 9: Tensile strength of $\phi 1.2$ mm wires. Corresponding relationship between sample number and hydrogen content: 1: $0.18 \mu\text{g/g}$, 2: $0.23 \mu\text{g/g}$, 3: $0.26 \mu\text{g/g}$, 4: $0.32 \mu\text{g/g}$, and 5: $0.38 \mu\text{g/g}$.

strength of the fracture. As a result, dislocations aggregate into microcracks to propagate continuously and became unstable, then caused the fracture. So, in terms of plastic strain, the specimen will not undergo much deformation before fracture.

The weak spots and the lower tensile strength would certainly cause the blocking and the instability while welding. Furthermore, the hydrogen could also enter the weld and affects the mechanical performance. As a consequence,

considering the microstructure and mechanical properties as well as the weldability of ER5183 wires, the hydrogen content should be controlled below $0.23 \mu\text{g/g}$.

4. Conclusions

The influence of the hydrogen content on the microstructure and mechanical properties of ER5183 wires was investigated. The conclusions are as follows:

- (1) The hydrogen content of the ER5183 wires ranged from 0.18 to $0.38 \mu\text{g/g}$. The wire with low hydrogen content ($0.18 \mu\text{g/g}$ and $0.23 \mu\text{g/g}$) occasionally breaks due to the issue of the production equipment and shows a ductile fracture surface. Higher content of hydrogen ($0.26 \mu\text{g/g}$, $0.32 \mu\text{g/g}$, and $0.38 \mu\text{g/g}$) could result in frequent fracture as well as three typical modes of irregular macroscopic fracture which might reduce production efficiency and wire quality.
- (2) The aggregated pores were observed in the microstructure of the $\phi 5.2$ mm wire with the hydrogen content of $0.38 \mu\text{g/g}$. Such defects may become the origin of cracks in subsequent processing and tensile tests.
- (3) There has been a gradual decline in the tensile strength of the $\phi 5.2$ mm wires with the increase of the hydrogen content. In the sample with the low hydrogen content, fractures with necking and less defects are found. In contrast, internal cracks and micropores appeared with the hydrogen content exceeded $0.23 \mu\text{g/g}$.
- (4) With the increase of the hydrogen content, the tensile strength and plastic strain rate of the $\phi 1.2$ mm wire decrease. Unstable crack propagation occurs in the welding wire with the high hydrogen content (higher than $0.23 \mu\text{g/g}$) during deformation, which leads to the fracture.
- (5) To improve the microstructure and mechanical properties, the hydrogen content of ER5183 wires should be controlled below $0.23 \mu\text{g/g}$.

Data Availability

The data used to support the findings of this study are available from the corresponding author upon request.

Conflicts of Interest

The authors declare that they have no conflicts of interest.

Acknowledgments

This research was funded by the National Natural Science Foundation of China (Grant no. 51675269), The State Key Laboratory of Advanced Brazing Filler Metals and Technology (Zhengzhou Research Institute of Mechanical Engineering), China (Grant no. SKLABFMT201704), and the Priority Academic Program Development of Jiangsu Higher Education Institutions (PAPD).

References

- [1] B. Wang, S. Xue, C. Ma, J. Wang, and Z. Lin, "Study in wire feedability-related properties of Al-5Mg solid wire electrodes bearing Zr for high-speed train," *Metals*, vol. 7, no. 12, p. 520, 2017.
- [2] J. Yang, S. Xue, H. Liu et al., "Effects of silicon on microstructures and properties of Al-40Zn-xSi filler metal," *Rare Metal Materials and Engineering*, vol. 45, no. 2, pp. 333–338, 2016.
- [3] G. Peng, Y. Ma, J. Hu et al., "Nanoindentation hardness distribution and strain field and fracture evolution in dissimilar friction stir-welded AA 6061-AA 5A06 aluminum alloy joints," *Advances in Materials Science and Engineering*, vol. 2018, Article ID 4873571, 11 pages, 2018.
- [4] B. Wang, S. Xue, C. Ma, J. Wang, and Z. Lin, "Effects of porosity, heat input and post-weld heat treatment on the microstructure and mechanical properties of TIG welded joints of AA6082-T6," *Metals*, vol. 7, no. 11, p. 463, 2017.
- [5] Z. Xu, Z.-h. Zhao, G.-s. Wang, C. Zhang, and J.-z. Cui, "Microstructure and mechanical properties of the welding joint filled with microalloying 5183 aluminum welding wires," *International Journal of Minerals, Metallurgy, and Materials*, vol. 21, no. 6, pp. 577–582, 2014.
- [6] S. M. Myers, M. I. Baskes, H. K. Birnbaum et al., "Hydrogen interactions with defects in crystalline solids," *Reviews of Modern Physics*, vol. 64, no. 2, pp. 559–617, 1992.
- [7] T. Cho, D. Delgado-Hernandez, K.-H. Lee, B.-J. Son, and T.-S. Kim, "Bayesian correlation prediction model between hydrogen-induced cracking in structural members," *Metals*, vol. 7, no. 6, p. 205, 2017.
- [8] C. Panagopoulos and P. Papanayiotou, "The influence of cathodic hydrogen charging on the mechanical behaviour of Al-4Zn-1Mg alloy," *Journal of Materials Science*, vol. 30, no. 13, pp. 3449–3456, 1995.
- [9] G. Lu, Q. Zhang, N. Kiousis et al., "Hydrogen-enhanced local plasticity in aluminum: an ab initio study," *Physical review letters*, vol. 87, no. 9, article 095501, 2001.
- [10] G. Gou, M. Zhang, H. Chen, J. Chen, P. Li, and Y. P. Yang, "Effect of humidity on porosity, microstructure, and fatigue strength of A7N01S-T5 aluminum alloy welded joints in high-speed trains," *Materials & Design*, vol. 85, pp. 309–317, 2015.
- [11] G. Lu and E. Kaxiras, "Hydrogen embrittlement of aluminum: the crucial role of vacancies," *Physical Review Letters*, vol. 94, no. 15, p. 155501, 2005.
- [12] E. P. Georgiou, J.-P. Celis, and C. N. Panagopoulos, "The effect of cold rolling on the hydrogen susceptibility of 5083 aluminum alloy," *Metals*, vol. 7, no. 11, p. 451, 2017.
- [13] H. Yu, Y. Xu, J. Song, J. Pu, X. Zhao, and G. Yao, "On-line monitor of hydrogen porosity based on arc spectral information in Al-Mg alloy pulsed gas tungsten arc welding," *Optics & Laser Technology*, vol. 70, pp. 30–38, 2015.
- [14] S.-L. Chou and W.-T. Tsai, "Effect of grain size on the hydrogen-assisted cracking in duplex stainless steels," *Materials Science and Engineering: A*, vol. 270, no. 2, pp. 219–224, 1999.
- [15] R. C. Picu and D. Zhang, "Atomistic study of pipe diffusion in Al-Mg alloys," *Acta Materialia*, vol. 52, no. 1, pp. 161–171, 2004.



Hindawi
Submit your manuscripts at
www.hindawi.com

